

Realistic Implementation of Massive Yang Mills for ρ and a_1 Mesons

Paul M. Hohler* and Ralf Rapp†

*Cyclotron Institute and Department of Physics & Astronomy,
Texas A&M University, College Station, Texas 77843-3366, USA*

(Dated: June 20, 2021)

We revisit the massive Yang-Mills approach to implement axial-/vector mesons into the chiral pion Lagrangian. Employing the non-linear realization of chiral symmetry, we compute vector and axial-vector spectral functions. This includes, for the first time, a resummation of the ρ propagator in the a_1 selfenergy while maintaining a partially conserved axial-vector current (PCAC). A realistic ρ propagator, combined with a recent idea of a chirally invariant continuum in the vector and axial-vector channels, turns out to be critical to obtain a quantitative description of hadronic τ -decay data which has not been achieved before in local-gauge approaches to the chiral lagrangian. The thus obtained model provides a realistic basis to rigorously address the long-standing question of chiral symmetry restoration in the context of dilepton data in heavy-ion collisions.

Chiral effective theories are a successful and widely used tool to describe the low-energy limit of Quantum Chromodynamics (QCD) dominated by pions [1]. Several approaches have been pursued to extend the chiral Lagrangian by including the light vector (V) and axial-vector (AV) mesons, ρ and a_1 . A theoretically appealing framework is their implementation as local gauge bosons of the chiral group, $SU(2)_L \times SU(2)_R$, with explicit mass terms [2]. The universality of the gauge principle limits the free parameters while recovering the phenomenologically successful concept of vector meson dominance (VMD). Two leading realizations of this idea are the massive Yang-Mills (MYM) [3] and hidden local symmetry (HLS) [4, 5] schemes which turn out to be on-shell equivalent.

Early studies using tree-level MYM were successful in reproducing basic decay properties of ρ and a_1 mesons (once so-called non-minimal terms were included) [3, 6, 7], but recent precision data for axial-/vector spectral functions from hadronic τ decays [8, 9] pose more stringent constraints, and require loop-level calculations. These lead to several problems for MYM; *e.g.*, in the AV channel, the $a_1 \rightarrow \rho\pi$ width develops a zero in the experimentally accessible region, followed by a rapid growth at higher energies. Furthermore, the basic chiral coupling of the a_1 to external electro-weak (EW) fields entails a lack of strength in the AV spectral function. These issues have hampered attempts to describe the τ -decay data. Within HLS, extensive 1-loop calculations have been carried out, showing good agreement with many decay branchings [5], but a comparison to the experimental spectral functions is not available.

Recent investigations have therefore either given up on the local implementation of the gauge group in favor of a global one [10, 11], or abandoned the notion of ρ and a_1 as gauge bosons [12], thus decoupling their role as chiral partners. A global implementation removes constraints between couplings of different terms in the effective Lagrangian. The added freedom allows for a successful fit of the AV spectral function to τ data while preserving chiral

symmetry at the 1-loop level [10], or to achieve a good description of a wide range of light-meson properties at tree level [11]. In Ref. [12], the a_1 is dynamically generated from $\rho\pi$ interactions which also allows for a good fit of the AV τ -decay data. However, as we will show below, it is also possible to resolve the problems within MYM.

In this letter, we implement two novel aspects into MYM: a fully dressed ρ propagator in the a_1 selfenergy and a chirally invariant high-energy continuum. Preserving chiral symmetry is challenging within the dressing procedure. We develop criteria by which particular vertex correction diagrams can be identified and included so as to preserve the chiral properties. In practice, the broad ρ smears out the energy dependence of the a_1 width, thus eliminating the troublesome zero. A universal perturbative continuum was recently suggested in a phenomenological application of V and AV spectral functions to QCD and Weinberg sum rules [13], and was found to extend into the a_1 peak region. This extra strength further helps in arriving at a quantitative description of the measured spectral functions within MYM.

The MYM Lagrangian with non-minimal terms reads

$$\begin{aligned} \mathcal{L}_{\text{MYM}} = & \frac{\tilde{f}_\pi^2}{8} (\text{Tr}[D_\mu U^\dagger D^\mu U] + \tilde{m}_\pi^2 \text{Tr}[U + U^\dagger - 2]) \\ & - \frac{1}{2} \text{Tr}[F_L^2 + F_R^2] + m_0^2 \text{Tr}[A_L^2 + A_R^2] \\ & - i\xi \text{Tr}[D_\mu U D_\nu U^\dagger F_L + D_\mu U^\dagger D_\nu U F_R] \\ & + \gamma \text{Tr}[F_L U F_R U^\dagger], \end{aligned} \quad (1)$$

where the pion fields $\pi = \pi^a \tau^a / \sqrt{2}$ emerge from expanding the nonlinear realization of the field $U = \exp[2i/F_\pi \pi]$. The covariant derivative is defined via the gauge coupling, g , and the gauge bosons, $A_{L/R} = A_{L/R}^a \tau^a / \sqrt{2}$, as

$$D_\mu U = \partial_\mu U - ig(A_{L\mu} U - U A_{R\mu}). \quad (2)$$

The ρ and a_1 fields are identified as the vector and axial-vector combinations of the gauge bosons according to

$$\begin{aligned} \rho_\mu &= \kappa_v (A_{L\mu} + A_{R\mu}) \\ a_\mu &= \kappa_a (A_{L\mu} - A_{R\mu}), \end{aligned} \quad (3)$$

where $\kappa_{v/a} = (1 \mp \gamma)^{-1/2}$ are field renormalizations needed to recover the kinetic terms of the meson fields. The chiral and gauge symmetries are explicitly broken by mass terms for the physical fields. The shift $a_\mu \rightarrow a_\mu + \alpha Z_\pi \partial_\mu \pi$ removes the unphysical $a_\mu \partial_\mu \pi$ coupling. The pion field renormalization, Z_π , recovers the pion kinetic term. This also renormalizes the pion decay constant, $\tilde{f}_\pi = F_\pi Z_\pi$, and the pion mass, $\tilde{m}_\pi = M_\pi/Z_\pi$, with the physical values $F_\pi=131$ MeV and $M_\pi=139.6$ MeV.

The theory is coupled to external EW fields by gauging them under the same groups as the mesons. The EW gauge couplings are fixed by the pion charge. This leaves four parameters in the theory: the hadronic gauge coupling g , the bare mass m_0 , and the two non-minimal couplings γ and ξ . They can be traded for the phenomenologically more pertinent set of the single- and three-derivative $\rho\pi\pi$ couplings, $g_{\rho\pi\pi}$ and $g_{\rho\pi\pi}^{(3)}$, and bare ρ and a_1 masses, M_ρ and M_{a_1} . The Lagrangian is expanded to generate the vertices of the physical fields in terms of these four parameters.

We define the axial-/vector spectral functions as $\rho_{V,A} = -\text{Im}\Pi_{V,A}^T/\pi$ in terms of the 4-D transverse current-current correlators $\Pi_{V,A}^T$. Since the mesons and external fields are gauge bosons of the same group, the imaginary part of the correlator can be expressed in terms of the propagator $D_{V,A}^T$ as

$$\rho_{V,A} = -C_{V,A} \text{Im} D_{V,A}^T/\pi, \quad (4)$$

with axial-/vector meson dominance-like couplings

$$C_V = \frac{M_\rho^4}{g_{\rho\pi\pi}^2}, \quad C_A = \frac{M_a^2 M_\rho^2}{g_{\rho\pi\pi}^2 Z_\pi^2}. \quad (5)$$

Note that (A)VMD is not *a priori* assumed in the coupling of the EW fields, but is recovered for the spectral function due to gauge symmetry.

A simple estimate with the above relations reveals the problem of lacking strength in the AV channel. From the τ -decay data (*cf.* Fig. 4 below), the ratio of peak heights between V and AV spectral functions is $\rho_A(M_{a_1}^2)/\rho_V(M_\rho^2) \sim 1/3$. However, evaluating Eq. (4) with physical widths $\Gamma_\rho \simeq 150$ MeV, $\Gamma_{a_1} \simeq 450$ MeV and masses $M_{a_1}^2 \simeq Z_\pi^2 M_\rho^2 \simeq 2M_\rho^2$, yields this ratio by a factor of $\sim \sqrt{2}$ too low (more for larger a_1 width). In global models, where the external fields and the axial-/vector mesons are not gauge bosons of the same group, the spectral functions are not constrained as in Eq. (4).

We start out by calculating the V and AV selfenergies figuring into the propagators to 1-loop order including all diagrams as shown in Fig. 1. We do not consider the πa_1 loop in the vector channel as its threshold is well above the ρ mass. This requires that, in order to preserve gauge symmetry, only part of the π -tadpole in the vector channel be included. The divergent loops are regulated using dimensional regulation and suitable counter

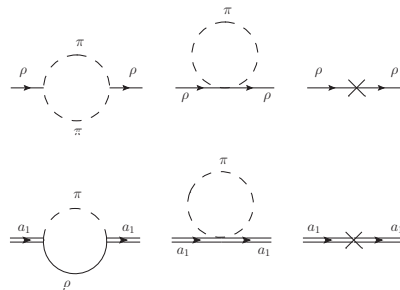


FIG. 1: Feynman diagrams used to calculate the ρ (upper panel) and a_1 (lower panel) selfenergies (crosses denote counter terms).

terms based on the Lagrangian, thus preserving chiral symmetry. Some of the counter terms are fixed to renormalize M_π and F_π to their physical values while others aid in fitting the spectral functions to experimental data, corresponding to six additional free parameters.

The resulting energy dependence of the $a_1 \rightarrow \rho\pi$ width, $\Gamma_{a_1 \rightarrow \rho\pi}(s) = -\text{Im}\Sigma_{a_1}^T(s)/\sqrt{s}$, reveals another problem, as a zero at an energy near the physical a_1 mass develops, *cf.* the dashed line in Fig. 2. To alleviate this issue, we will in the following incorporate the fully dressed ρ propagator into the AV loop calculation. This is expected to smear out the energy dependence and thus fill in the valley created by the zero. However, a naive resummation will not preserve chiral symmetry, requiring hitherto unknown vertex corrections.

Let us investigate the partial conservation of the axial current (PCAC). At tree level, the axial Noether current is given in terms of the W , a_1 , and π fields as

$$J_A^\mu = \alpha W^\mu + \beta a^\mu + \gamma \partial^\mu \pi, \quad (6)$$

where the couplings to the axial current are given by

$$\alpha = \frac{1}{2} F_\pi^2 Z_\pi^2, \quad \beta = \frac{1}{2} g_{\rho\pi\pi} F_\pi^2 Z_\pi \frac{M_{a_1}}{M_\rho}, \quad \gamma = -\frac{F_\pi}{\sqrt{2}}. \quad (7)$$

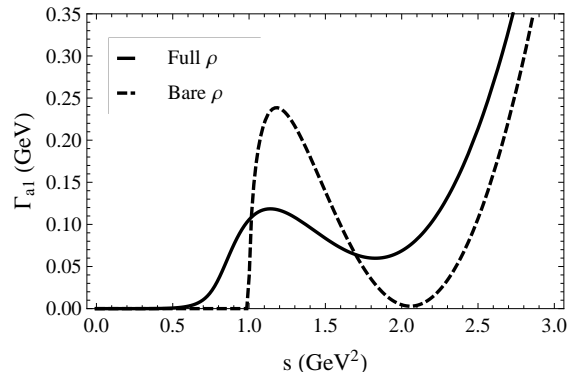


FIG. 2: Energy dependence of $\Gamma(a_1 \rightarrow \rho\pi)$ with a fixed-mass ρ (dashed curve) and a resummed ρ propagator with vertex corrections (solid curve).

One can verify that this current satisfies PCAC.

At 1-loop level, multi-pion states contribute which render the Noether current more involved. We follow Refs. [10, 14] to infer a generalized form of PCAC from the first Weinberg sum rule [15],

$$\int \frac{(-\text{Im}\Pi_A^L)}{\pi s} ds = \frac{F_\pi^2}{2}, \quad (8)$$

where Π_A^L is the 4-D longitudinal axial current-current correlator. It is defined by considering all possible W - W transitions: the direct W selfenergy, Σ_{WW} , as well as W couplings through a_1 and/or π propagators,

$$\begin{aligned} \Pi_A^L &= \Sigma_{WW} + \frac{(\beta + \Sigma_{Wa})^2}{M_a^2 - \Sigma_{aa}^L} + \frac{p^2}{p^2 - M_\pi^2 - \Sigma_\pi} \\ &\times \left(-\frac{F_\pi}{\sqrt{2}} + \Sigma_{W\pi} - \frac{\Sigma_{a\pi}}{M_a^2 - \Sigma_{aa}^L} (\beta + \Sigma_{Wa}) \right)^2. \end{aligned} \quad (9)$$

The Σ_{ij} are selfenergies with external legs $i, j=a_1, \pi, W$; the pion selfenergy includes a direct contribution and one with an intermediate a_1 propagator,

$$\Sigma_\pi \equiv \Sigma_{\pi\pi} + \frac{p^2 \Sigma_{a\pi}^2}{M_a^2 - \Sigma_{aa}^L}. \quad (10)$$

One can now show that Eq. (8) is satisfied when the selfenergies obey the relations

$$\begin{aligned} \Sigma_{WW} &= \frac{\alpha^2}{\beta^2} \Sigma_{aa}^L, \quad \Sigma_{Wa} = -\frac{\alpha}{\beta} \Sigma_{aa}^L, \quad \Sigma_{W\pi} = \frac{\alpha}{\beta} \Sigma_{a\pi}, \\ \Sigma_{aa}^L &= \frac{\beta^2}{\gamma^2 p^2} \Sigma_{\pi\pi}, \quad \Sigma_{a\pi} = -\frac{\beta}{\gamma p^2} \Sigma_{\pi\pi}. \end{aligned} \quad (11)$$

(note their scaling with the tree-level couplings). The first three are a consequence of gauge symmetry, while the last two encode chiral symmetry. Let us therefore focus on the latter: our strategy is to use them as criteria to enforce PCAC.

At 1-loop level, where the ρ -meson figures with a “sharp” (bare) mass M_ρ in the $\pi\rho$ loops, the longitudinal selfenergies can be factored into a universal loop integral, $\bar{\Sigma}$, and vertex functions, v_{ij} , as

$$\Sigma_{aa}^L = v_{aa}(M_\rho^2) \bar{\Sigma}, \quad \Sigma_{a\pi} = v_{a\pi}(M_\rho^2) \bar{\Sigma}, \quad \Sigma_{\pi\pi} = v_{\pi\pi}(M_\rho^2) \bar{\Sigma}, \quad (12)$$

satisfying Eqs. (11). When using the full ρ propagator, D_ρ , the selfenergies still factorize, but the vertex functions now depend on both M_ρ and the off-shell ρ mass M (to be integrated over); *e.g.*, Σ_{aa}^L takes the form

$$\Sigma_{aa}^L = \int \frac{-\text{Im}D_\rho(M^2)}{\pi} v_{aa}(M_\rho, M) \bar{\Sigma} dM^2. \quad (13)$$

Since the v_{ij} generally depend differently on M and M_ρ , Eq. (11) is violated. However, it turns out that the inclusion of the vertex corrections depicted in Fig. 3 can

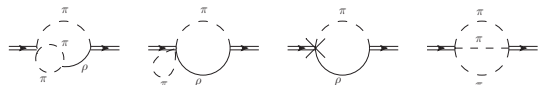


FIG. 3: Vertex correction diagrams to recover PCAC in the presence of a full ρ propagator. External legs are W , a_1 or π to generate the selfenergy Σ_{ij} . The first three diagrams show the corrections to the left-hand vertex while the complete set includes the corrections to the right-hand vertex and to both simultaneously. The ρ propagator in each diagram is the fully dressed one.

recover the structure of Eq. (12), *i.e.*, selfenergies factorized into the same $v_{ij}(M_\rho^2)$ as before and a different but universal loop integral, $\bar{\Sigma}^*$ (which now includes an additional M integration). This can be achieved by casting the first three diagrams into a vertex correction proportional to Σ_ρ , and then combining it with the “bare” 3π loop (last diagram in Fig. 3) where two pions are required to be in a relative P-wave. One also has to make a judicious choice of the 3π , $\rho 3\pi$ and counterterm couplings in Fig. 3, differing from the Lagrangian value. This is not unexpected since the use of the full ρ propagator implies a *partial* resummation in the first place.

The energy dependence of the $a_1 \rightarrow \rho\pi$ width with the dressed ρ propagator and associated vertex corrections resolves the problem of the zero, *cf.* solid line in Fig. 2. As an extra benefit, finite strength develops below the previously sharp $\rho\pi$ threshold. However, the concern over the high-energy behavior persists, which we address next.

On dimensional grounds, the two-derivative $a_1\rho\pi$ coupling and the ρ propagator render the a_1 selfenergy to scale as p^6 at high energies. Since the onset of this behavior is only slightly above the a_1 peak, the large width suppresses spectral strength in the AV spectral function causes it to fall off faster than the τ -decay data. We interpret this as an indication that the effective hadronic theory is breaking down, and additional physics is needed. In fact, this is precisely what has been deduced from a recent phenomenological analysis [13] of V and AV spectral functions, where a chirally invariant continuum has been postulated, parameterized following [16] as

$$\rho_{\text{cont}}(s) = \frac{1}{8\pi^2} \left(1 + \frac{\alpha_s}{\pi}\right) \frac{s}{1 + \exp[(E_0 - \sqrt{s})/\delta]}. \quad (14)$$

This carries significant strength into the a_1 peak region. When adopting this continuum in connection with our microscopic model, we are able to overcome the lacking-strength problem of MYM.

Our final fit to the τ -decay data [8], shown in Fig. 4, is obtained with the parameters $g_{\rho\pi\pi}=6.01$, $g_{\rho\pi\pi}^{(3)}=0.02 \text{ GeV}^{-2}$, $M_\rho=0.86 \text{ GeV}$, and $M_{a_1}=1.20 \text{ GeV}$, with an additional six counter terms to renormalize the theory. Note that $g_{\rho\pi\pi}^{(3)}$ is small as required for the effective theory to have a meaningful derivative expansion. The continuum parameters ($\alpha_s=0.5$, $E_0=1.5 \text{ GeV}$

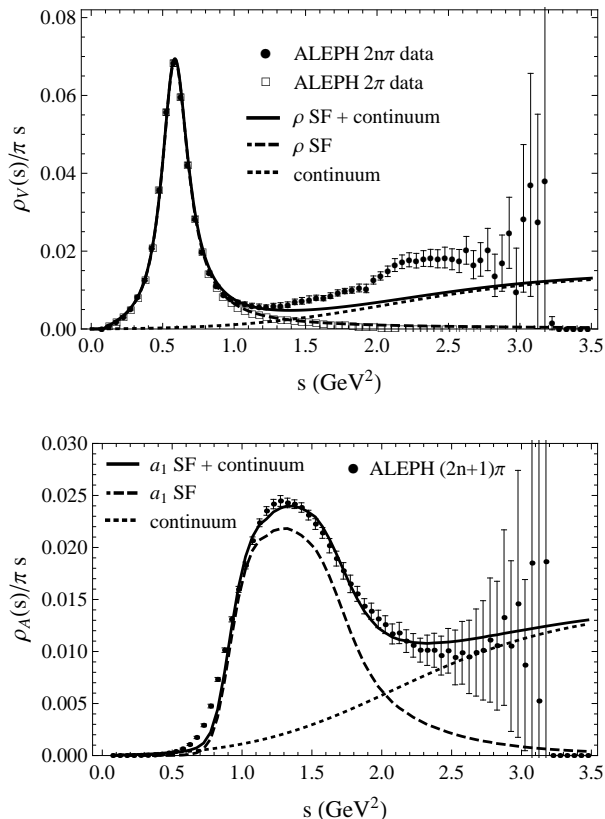


FIG. 4: Spectral functions in the vector (upper panel) and axial-vector (lower panel) channels calculated from MYM (dashed lines), supplemented with a chirally invariant continuum (dotted lines) and compared to τ -decay data [8].

and $\delta=0.2$ GeV) have been slightly varied compared to Ref. [13] to optimize the fit. Satisfactory agreement is found in both V and AV channels (excited states (ρ' and a_1') can be included to complete the fit [13]). We have checked that data for the P-wave $\pi\pi$ phase shifts as well as the pion electromagnetic formfactor are reproduced well. The calculated value for the radiative a_1 decay, $\Gamma_{a_1 \rightarrow \rho\gamma}=244$ keV is somewhat low compared to the available data extracted from proton-nucleus collisions (640 ± 246 keV) [17]. Our D/S ratio of -0.131 (evaluated at the physical a_1 mass, $\sqrt{s}=1.23$ GeV) is significantly enhanced over the tree level result; it approximately agrees with three of the four measurements reported by the Particle Data Group [18]. We have numerically verified that PCAC is satisfied through Eq. (8) at the sub 0.1% level, with the discrepancy scaling with M_π^2 , as expected.

We have conducted an analogous investigation within the linear realization of chiral symmetry (σ model). Using a sharp σ meson, the fit to the τ data preferred rather large masses ($m_\sigma \simeq 0.8$ GeV), but did not reach the quality as in the non-linear version. Whether a broad σ meson can improve on this remains to be seen.

To summarize, we have set up a non-minimal MYM approach where, for the first time, a resummed ρ propagator has been implemented while maintaining the chiral properties through suitably identified vertex corrections. This enabled us to overcome previous problems in a realistic description of the τ -decay data in the axial-vector channel. The effective hadronic theory decouples slightly above the a_1 peak, beyond which the recently introduced idea of a universal perturbative continuum aids in maintaining agreement with the experimental spectral functions. We believe that our work helps to re-establish MYM as a viable description of axial-/vector mesons in the chiral Lagrangian. This is particularly welcome in the context of dilepton spectra in heavy-ion collisions, where the in-medium vector channel (based on MYM) yields a quantitative description of available data. The implementation of the here constructed axial-vector spectral function into hadronic matter can thus serve as a quantitative framework to establish the long-sought connection to chiral symmetry restoration.

We thank H. van Hees for discussions. This work is supported by the U.S.-NSF grant no. PHY-1306359 and by the A.-v.-Humboldt Foundation (Germany).

* Electronic address: pmhohler@comp.tamu.edu

† Electronic address: rapp@comp.tamu.edu

- [1] J. Gasser and H. Leutwyler, *Annals Phys.* **158**, 142 (1984).
- [2] U. G. Meissner, *Phys. Rept.* **161**, 213 (1988).
- [3] H. Gomm, O. Kaymakcalan and J. Schechter, *Phys. Rev. D* **30**, 2345 (1984).
- [4] M. Bando, T. Kugo and K. Yamawaki, *Phys. Rept.* **164**, 217 (1988).
- [5] M. Harada and K. Yamawaki, *Phys. Rept.* **381**, 1 (2003).
- [6] C. Song, *Phys. Rev. C* **47**, 2861 (1993).
- [7] P. Ko and S. Rudaz, *Phys. Rev. D* **50**, 6877 (1994).
- [8] R. Barate *et al.* [ALEPH Collaboration], *Eur. Phys. J. C* **4**, 409 (1998).
- [9] K. Ackerstaff *et al.* [OPAL Collaboration], *Eur. Phys. J. C* **7**, 571 (1999).
- [10] M. Urban, M. Buballa and J. Wambach, *Nucl. Phys. A* **697**, 338 (2002).
- [11] D. Parganlija, F. Giacosa and D.H. Rischke, *Phys. Rev. D* **82**, 054024 (2010).
- [12] M. Wagner and S. Leupold, *Phys. Rev. D* **78**, 053001 (2008).
- [13] P.M. Hohler and R. Rapp, *Nucl. Phys. A* **892**, 58 (2012).
- [14] S. Weinberg, *The quantum theory of fields. Vol. 2: Modern applications*, Cambridge Univ. Pr. (1996).
- [15] S. Weinberg, *Phys. Rev. Lett.* **18** (1967) 507.
- [16] E. V. Shuryak, *Rev. Mod. Phys.* **65**, 1 (1993).
- [17] M. Zielinski *et al.*, *Phys. Rev. Lett.* **52**, 1195 (1984).
- [18] J. Beringer *et al.* (Particle Data Group), *Phys. Rev. D* **86**, 010001 (2012).